

See discussions, stats, and author profiles for this publication at: <https://www.researchgate.net/publication/266356145>

Machinery Performance Assessment Based on Records of Geographic Position

Article · January 2004

DOI: 10.13031/2013.17067

CITATIONS

8

READS

105

3 authors:



Viacheslav I Adamchuk

McGill University

235 PUBLICATIONS 6,091 CITATIONS

[SEE PROFILE](#)



Robert D Grisso

Virginia Tech (Virginia Polytechnic Institute and State University)

181 PUBLICATIONS 2,132 CITATIONS

[SEE PROFILE](#)



Michael F Kocher

University of Nebraska at Lincoln

70 PUBLICATIONS 1,355 CITATIONS

[SEE PROFILE](#)

Some of the authors of this publication are also working on these related projects:



Application of Variable-Rate Irrigation Technology to Conserve Water and Improve Crop Productivity [View project](#)



Performance measurement of three-point mounted implement guidance systems [View project](#)



*The Society for engineering
in agricultural, food, and
biological systems*



*The Canadian Society for
Engineering in Agricultural,
Food, and Biological Systems*

An ASAE/CSAE Meeting Presentation

Paper Number: 041149

Machinery Performance Assessment Based on Records of Geographic Position

Viacheslav I. Adamchuk

Department of Biological System Engineering, University of Nebraska-Lincoln
212 L.W. Chase Hall, Lincoln, NE 68583-0726, USA, vadamchuk2@unl.edu

Robert D. Grisso

Department of Biological System Engineering, Virginia Tech,
211 Seitz Hall, Blacksburg, VA 24061-0303, USA, rgrisso@vt.edu

Michael F. Kocher

Department of Biological System Engineering, University of Nebraska-Lincoln
205 L.W. Chase Hall, Lincoln, NE 68583-0726, USA, mkocher1@unl.edu

**Written for presentation at the
2004 ASAE/CSAE Annual International Meeting
Sponsored by ASAE/CSAE
Fairmont Chateau Laurier, The Westin, Government Centre
Ottawa, Ontario, Canada
1 - 4 August 2004**

Abstract. *Logging the geographic coordinates of agricultural machinery measured using a Global Positioning System (GPS) receiver is a common practice in site-specific crop management. Yield, fertilizer application and seed placement maps are useful data to make agronomic decisions. In addition, the travel path itself reveals valuable information about machinery performance. Odd field shapes, obstacles, or contour farming frequently require operators to increase the complexity of maneuvering during different field operations. This usually reduces field efficiency. In this work, a methodology was developed to parameterize the spatially variable characteristics of traffic patterns and to define field areas with significant reduction in field efficiency. Geographic positions recorded during harvesting of a field with complex shape were used to illustrate the method developed. The information obtained can be used either to optimize the traffic patterns, if possible, or to reevaluate the potential profitability of field areas with different degrees of machinery maneuvering complexity.*

Keywords: *field efficiency, machinery management, geo-referenced data.*

The authors are solely responsible for the content of this technical presentation. The technical presentation does not necessarily reflect the official position of ASAE or CSAE, and its printing and distribution does not constitute an endorsement of views which may be expressed. Technical presentations are not subject to the formal peer review process, therefore, they are not to be presented as refereed publications. Citation of this work should state that it is from an ASAE/CSAE meeting paper. EXAMPLE: Author's Last Name, Initials. 2004. Title of Presentation. ASAE/CSAE Meeting Paper No. 04xxxx. St. Joseph, Mich.: ASAE. For information about securing permission to reprint or reproduce a technical presentation, please contact ASAE at hq@asae.org or 269-429-0300 (2950 Niles Road, St. Joseph, MI 49085-9659 USA).

Introduction

The implementation of precision agriculture practices in modern crop production generates large amount of records containing the coordinates of agricultural machinery location during various field operations. Historically, these coordinates were used to locate the physical value associated with the corresponding field operation (i.e. crop yield, fertilizer application rate, implement draft, etc.). Development and processing of numerous layers of spatial data has been the major approach in utilizing geographical coordinates. In addition, a continuous log of the geographic coordinates of agricultural machinery within a field provides valuable information on machinery performance that can (and probably should) be used to determine the spatially variable cost of machinery operation. According to MAX[®] (Farming for MAXimum Efficiency, Conservation Technology Information Center, West Lafayette, Indiana), machinery operation can be as high as 25% of the total cost of crop production. Since field geometry frequently causes farmers to invest greater effort in operating within non-rectangular areas of the field (waterways, terraces, etc.), uniform distribution of the machinery operation cost across the entire field area can provide misleading outputs when developing profitability maps.

Field capacity and field efficiency (ASAE, 2002a) are two primary parameters used to evaluate machinery performance. While field capacity represents the area of land processed in given time, field efficiency is defined as the ratio between effective and theoretical field capacities and relates estimated and actual time required to complete field operation. In the past, both values were evaluated on a field basis or simply obtained using a reference table (ASAE, 2002b). Thus, Renoll (1981) was using a conventional recording method (stop watch and a clipboard) to determine field machinery performance. Alternatively, Grisso et al. (2002) as well as Taylor et al. (2002) were using records of machinery location determined with a Global Positioning System (GPS) receiver. They proved geospatial field records to be an effective way of evaluating overall machinery performance. In a study conducted by Grisso et al. (2004), the position of farm machinery logged during harvesting and planting operations were used not only to evaluate field efficiency but also to define parameters representing the complexity of traffic patterns. Steering angle, steering angle per distance traveled, steering rate, and radius of curvature were the primary indices introduced. Their field averages indicated some correspondence with the overall field efficiency when processing fields with various types of traffic patterns.

The primary objective of this study was to explore opportunities for using farm machinery position records to evaluate the spatial variability of machinery performance. Specifically, analytical tools to construct maps representing the variability of machinery usage in various field locations were to be developed.

Materials and Methods

There are a number of approaches available to process machinery position log files. They include different filters and geometrical transformations. However, in every case, the efficiency of farm machinery operation can be affected by three factors: 1) travel speed, 2) effective swath width, and 3) field traffic pattern. The position logging interval is assumed to be constant, but can affect the results reported as well. In this work, area coverage was used as the primary parameter in combining all influential factors.

Algorithm Development

To develop an algorithm for traffic pattern processing, the following assumptions were made: 1) the entire log was created using a fixed time interval, and 2) the resulting map should show area coverage produced by the machine in every field location. It was also assumed that the coverage of farm machinery can be simplified by a sequence of rectangular segments defined by the recorded geographic positions. Figure 1 illustrates a route represented by four points: A, B, C, and D. Each segment of this route can be represented either as a sequence of rectangles with constant width (w) and variable distance (d) or with constant width and fixed distance (d_f). Variable distance is used to determine actual coverage provided by the machine, and fixed distance can be used to assess deviation from potential coverage if constant travel speed was maintained while operating along the same route. More complex segments incorporating travel pass curvature can also be used to better represent the actual coverage.

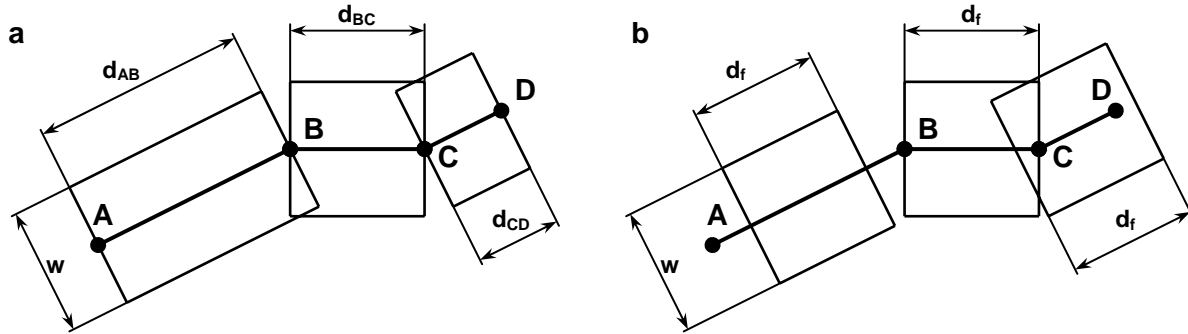


Figure 1. Simplified segments of a travel route ABCD using a) variable (actual) travel speed and b) constant (theoretical) speed of operation.

To assure that every field location has a defined coverage, an equally spaced grid with minimum and maximum coordinates corresponding to the maximum extents of the field was used to construct the output. Figure 2 shows such a grid representing a section of a field with points corresponding to the route A-B-C-D. Every linear segment of the route was represented by the rectangular area coverage, and was related to the grid cells overlapped by this rectangle. To illustrate the calculation procedure, a linear segment between points B with coordinates (x_1, y_1) and C (x_2, y_2) was considered. Values x and y corresponded to easting and northing coordinates, expressed in linear units (m). The simplified coverage segment was represented by a rectangle with width (w) corresponding to the physical width of the implement and length (d) calculated as the distance between B and C:

$$d = \sqrt{(x_2 - x_1)^2 + (y_2 - y_1)^2} \quad (1)$$

The center of this rectangle $O(x_0, y_0)$ had coordinates:

$$\begin{aligned} x_0 &= \frac{x_1 + x_2}{2} \\ y_0 &= \frac{y_1 + y_2}{2} \end{aligned} \quad (2)$$

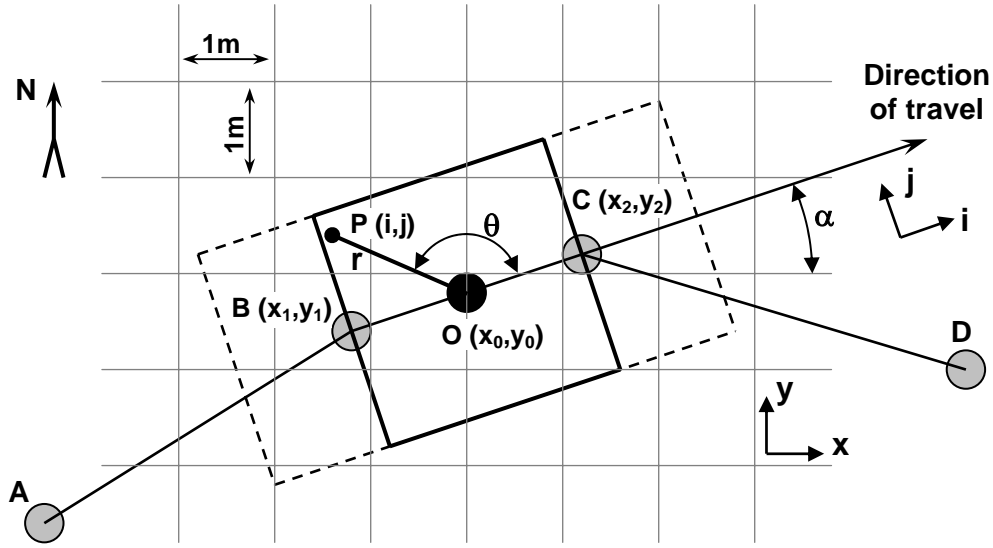


Figure 2. Area coverage computation diagram.

On the other hand, the same rectangular coverage area was viewed as an array of infinite number of points P with local coordinates i and j . It was assumed that the direction of i corresponded to the direction of travel and the center of rectangle O had both i and j equal to zero. Therefore, coordinate i changed from $-d/2$ to $d/2$, and j from $-w/2$ to $w/2$. If increments of i and j coordinates are set to a finite number, a defined array of points $P(i, j)$ can be obtained. In this work the increment for both coordinates was set 10 times smaller (0.1 m) than the side of a square grid cell (1 m). This allowed the total of $100 \cdot d \cdot w$ points P arranged in a $10d$ by $10w$ array to represent the entire rectangle. Through a looping routine illustrated in Figure 3, each point was assigned to one of the predefined grid cells using x and y coordinates. In the result, 100 points P were assigned to grids completely covered by the rectangle. Non-covered grid cells remained with zero point counts, and, consecutively, partially covered cells were associated with a number of points between 1 and 99, for a given rectangle.

Both (x, y) and (i, j) coordinate systems were related using an angle α between the travel direction and the positive x axis:

$$\begin{aligned}
 \alpha &= \frac{\pi}{2} && \text{for } x_1 = x_2 \text{ and } y_1 < y_2 \\
 \alpha &= \frac{3\pi}{2} && \text{for } x_1 = x_2 \text{ and } y_1 > y_2 \\
 \alpha &= \arctan\left(\frac{y_2 - y_1}{x_2 - x_1}\right) && \text{for } x_1 < x_2 \\
 \alpha &= \pi + \arctan\left(\frac{y_2 - y_1}{x_2 - x_1}\right) && \text{for } x_1 > x_2
 \end{aligned} \tag{3}$$

In addition to local rectangular coordinates i and j , every point P was defined using local polar coordinates r and θ with respect to the center of the rectangle O and the positive direction of i . In our algorithm, points with coordinates $i = 0$ or $j = 0$ were avoided to reduce the number of logical operators. Therefore:

$$r = \sqrt{i^2 + j^2} \quad \text{and} \quad \begin{aligned} \theta &= \arctan\left(\frac{j}{i}\right) \quad \text{for } i > 0 \\ \theta &= \pi + \arctan\left(\frac{j}{i}\right) \quad \text{for } i < 0 \end{aligned} \quad (4)$$

To determine coordinates (x, y) of a grid cell associated with a point $P(r, \theta)$, the following equations were used:

$$\begin{aligned} x &= \text{round}(x_0 + r \cos(\theta + \alpha)) \\ y &= \text{round}(y_0 + r \sin(\theta + \alpha)) \end{aligned} \quad (5)$$

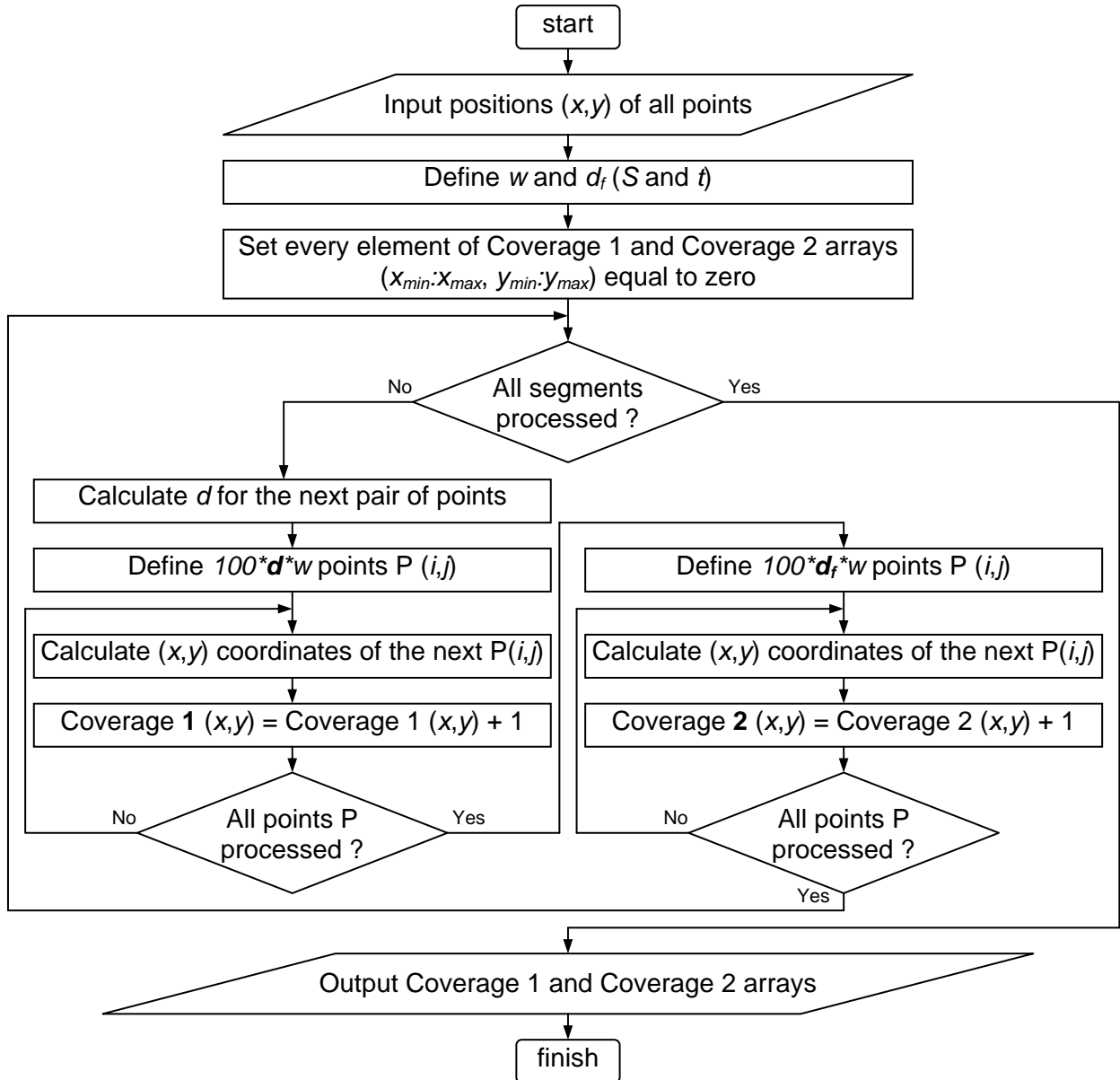


Figure 3. Algorithm for calculating Coverage 1 and Coverage 2 data layers.

After running the algorithm shown in Figure 3, a two-dimensional array Coverage 1 with values corresponding to percent coverage for each square meter of the field was obtained. This array represents the physical coverage of each field location. Efficiency, on the other hand, can be related to the coverage that would have been achieved if travel speed remained constant across the entire field (Coverage 2). Therefore, a fixed (theoretical) distance between two consecutive records (d_f), also shown in Figure 1, was defined as the product of the average operation travel speed (S), and the position logging interval (t):

$$d_f = S \cdot t \quad (6)$$

The described algorithm was executed using Matlab® 6 (The MathWorks, Natick, Massachusetts). The input delimited text file contained three columns (easting - x , northing - y , and time interval between two consecutive records). The output file had four columns containing coordinates x and y for the center of each grid cell as well as corresponding Coverage 1 and Coverage 2. Coverage 1 was calculated using the variable (actual) distance traveled d (assuming a continuous route). On the other hand, the fixed (theoretical) distance traveled d_f was determined and used while calculating the values corresponding to Coverage 2.

Field Data

To illustrate the algorithm output, an agricultural field with a complex shape (Field R1, Rogers Memorial Farm, Eagle, Nebraska) with a total area of 4.24 ha was selected. A soybean harvesting operation was used. The combine header was 4.6 m (15 ft) wide ($w = 4.6$ m). The total of 6.44 Mg of soybean with average yield of 1.52 Mg/ha was harvested and removed from the field using three unloads. Two data files were simultaneously generated. A PF3000™ (Ag Leader Technology, Inc., Ames, Iowa) yield monitor with an add-on AgLeader 3100 GPS receiver (beacon differential correction) was used to collect the yield-related information while harvesting. The position of the center of the combine was recorded in 4 s (0.25 Hz) intervals with the header down (during harvesting only). A standard begin/end of row delay filter was applied. In addition, a GPS 16 (Garmin International Inc., Olathe, Kansas) receiver with WAAS differential correction was placed 1.1 m to the right of the Ag Leader antennae. The receiver output was separately recorded with 1 s (1 Hz) interval from the beginning to the end of field harvesting (including stops, maneuvering, and unloads).

Initial data processing included conversion of geographic longitude and latitude into the local rectangular coordinates according to Adamchuk (2001), and correcting the position of the Garmin GPS 16 receiver. Figure 2 illustrates the continuous position log (Garmin receiver) and positions recorded by the yield monitor (Ag Leader GPS receiver). Continuous log contains records from the beginning to the end of harvesting, while yield monitor output had non-harvesting locations excluded.

The algorithm developed can be applied to any logging of a travel route. However, the meaning of Coverage 1 and Coverage 2 values changes depending on which positions are excluded from the input file. It is critical to identify whether turns, stops, and unexpected field maneuvering are included in the log file or not. In our study, the continuous (non-stop) log was used to analyze spatial variability of combining efficiency. The yield monitor recordings were used primarily to define the operation parameters during field harvesting. One such parameter was the average harvesting speed (S), which was found to be 1.4 m/s. Therefore, $d_f = 1.4$ m (for continuous log with $t = 1$ s).

The maps of Coverage 1 and Coverage 2 reveal the spatial variability of machinery performance. However, this information should be converted into the conventional terms of

capacity, efficiency and cost in order to be incorporated into the decision-making strategy. From the overall evaluation of the recorded data, the field with an actual area of 4.24 ha was harvested in 2.78 h. This resulted in an effective capacity of 4.24 m²/s (1.53 ha/h). On the other hand, the theoretical capacity (header width times average harvesting speed) was 6.44 m²/s (2.32 ha/h). The ratio of effective and theoretical field capacities determined that the field efficiency was 0.66. In addition, according to Jose and Brown (2002), \$49.42/ha (\$20/acre) is the most common farm custom rate for soybean harvesting. Therefore, the total cost of this operation was \$210.

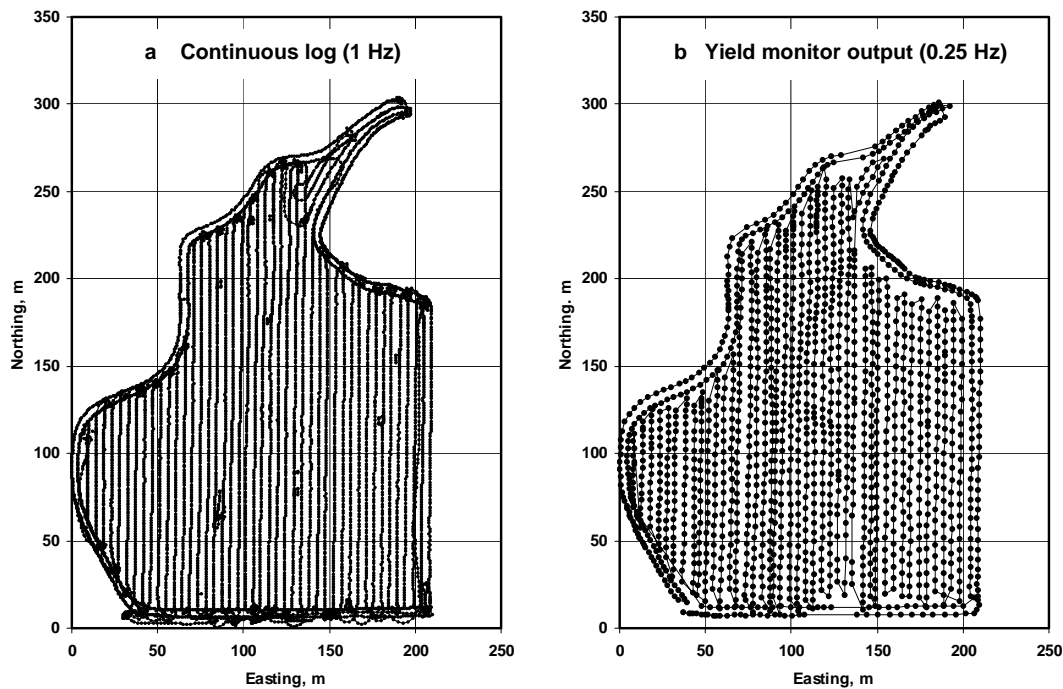


Figure 4. Combine geographic positions logged a) continuously and b) while harvesting.

Alternatively, analysis of the algorithm outputs revealed that the sum of all non-zero values compositing Coverage 1 and Coverage 2 arrays resulted in 5.80 and 6.42 ha, respectively. This means that the 37% increase in the Coverage 1 area resulted from overlaps during maneuvering and reduced width of cut. Correspondingly, the 51% increase in the Coverage 2 area was caused by both overlaps and overestimation of travel speed (including stops). The average travel speed was 1.26 m/s (90% of average harvesting speed). Therefore, the overall field efficiency of 0.66 (same as the ratio of actual field area to the sum of the Coverage 2 map) can be separated into effects of the efficiency varying due to the combine route and efficiency varying due to inconsistent travel speed. The second effect can be defined as the ratio of Coverage 1 to Coverage 2 (0.90).

Results and Discussion

Figure 5 shows maps of Coverage 1 and 2 produced using continuous log (Figure 4a). According to the color scheme, < 75% coverage corresponds to the areas with potential skips (Coverage 1 and 2) and increased speed operation (Coverage 2). Similarly, > 125% coverage indicates the potential for overlaps, including multi-passes and stops (Coverage 1 and 2), and

slow downs (Coverage 2). The rest of the field indicates areas with normal coverage (Coverage 1 and 2) and average harvesting speed (Coverage 2). The Coverage 1 map indicates the physical presence of the harvester. The Coverage 2 map also indicates areas with travel speed deviating from the average harvest speed. Since the size of a grid was 1 m² (smaller than the GPS receiver accuracy), some indication of potential skips and overlaps could result from imprecise measurement of the harvester position. The rectangular representation of route segments between two consecutive points during high-speed turns could present additional noise. Map smoothing using conventional interpolation techniques could improve the visual appearance of these maps.

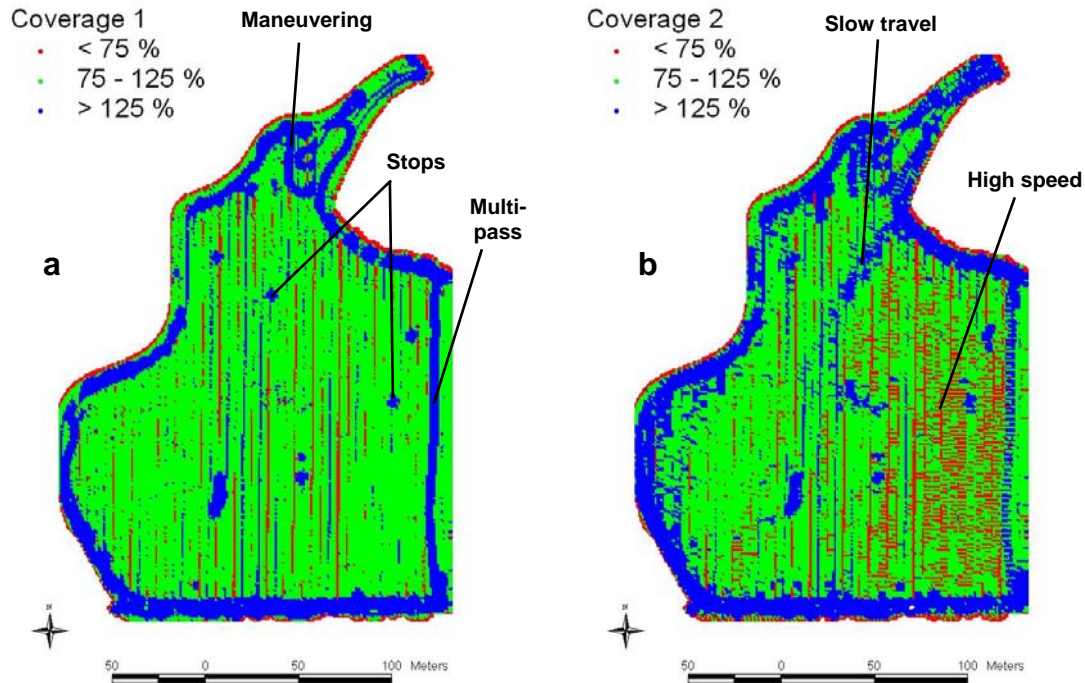


Figure 5. Grid of field coverage calculated using variable (a) and fixed (b) distance between two consecutive points.

Figure 6 illustrates a couple of categorical maps that can be produced based on Coverage 1 and Coverage 2. Another field coverage map (Figure 6a) was derived from Coverage 1 as the inverse of all grid cells with higher than 100% coverage. It indicates coverage efficiency, which was categorized into three intervals: < 0.5 – maneuvering, 0.5-0.9 – overlaps, and 0.9-1.0 – normal coverage. This map can be used to improve traffic patterns through optimization of the harvester route during non-harvest portions of operation (unloads, turns, etc.).

Since the Coverage 2 map was developed based on the assumption of a constant speed, dividing by the theoretical field capacity resulted in time spent in each field location. If time is used as the major indicator of investment, the total cost of harvesting can be redistributed according to the time (\$210 distributed over 2.78 h equal to \$0.021/s). Figure 6b illustrates a cost of harvesting map categorized with < \$40/ha corresponding to the low cost, \$40-60/ha – average, \$60-100/ha – high, and > \$/100/ha – very high cost of harvesting. This map can be used to calculate profitability maps based on the spatially variable cost of field operations. If profit map values are negative in particular field areas (such as the northern portion of the illustrated field), alternative traffic pattern and/or land usage should be considered.

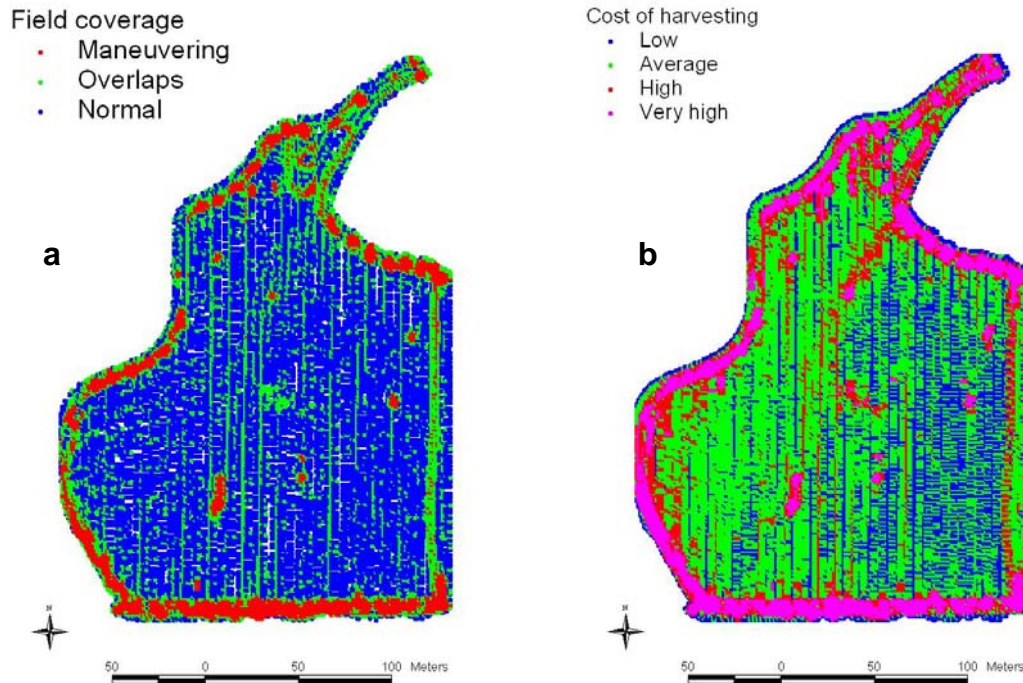


Figure 6. Categorical maps of field coverage (a) and cost of harvesting (b).

Effective field capacity and field efficiency can be calculated to evaluate overall performance as well as to investigate speed variation effects. Thus, Coverage 1 divided by time (same as time used calculate cost of harvesting) corresponds to the physical coverage of the square grid area in a unit of time. After dividing by the corresponding average field capacity ($5.82 \text{ m}^2/\text{s}$), a map of field efficiency due to the variable speed effect can be constructed (Figure 7a). At least 50% of the covered grid cells were used in these calculations. Higher than 1 speed field efficiency represents areas with relatively high speed of operation, while grid cells with less than 1 speed field efficiency were located where the actual coverage area was smaller than what potentially could be covered in the same time. This map removes the effect of maneuvering, and can be used to determine locations of the actual slow-downs.

On the other hand, overall field efficiency, the ratio between actual (area of a grid cell divided by time) and theoretical ($6.44 \text{ m}^2/\text{s}$) field efficiencies, indicates the overall field performance (Figure 7b). This map is associated with the cost map and can be used to derive an overall judgment about potentially abusing areas of the field (low efficiency - high cost). Further employment of these data sets is still under consideration and logical routines analyzing the outputs are needed. However, we believe that there two major strategies that can be pursued. First, the areas with relatively high loss of field efficiency due to a systematic non-productive machinery operation (extra turns, travel around obstacles, point rows, etc.) can be evaluated to seek more effective traffic pattern. Second, field efficiency expressed in monetary terms can be used to conduct evaluation of potential profitability in different field areas while accounting for spatially inconsistent cost of field operations.

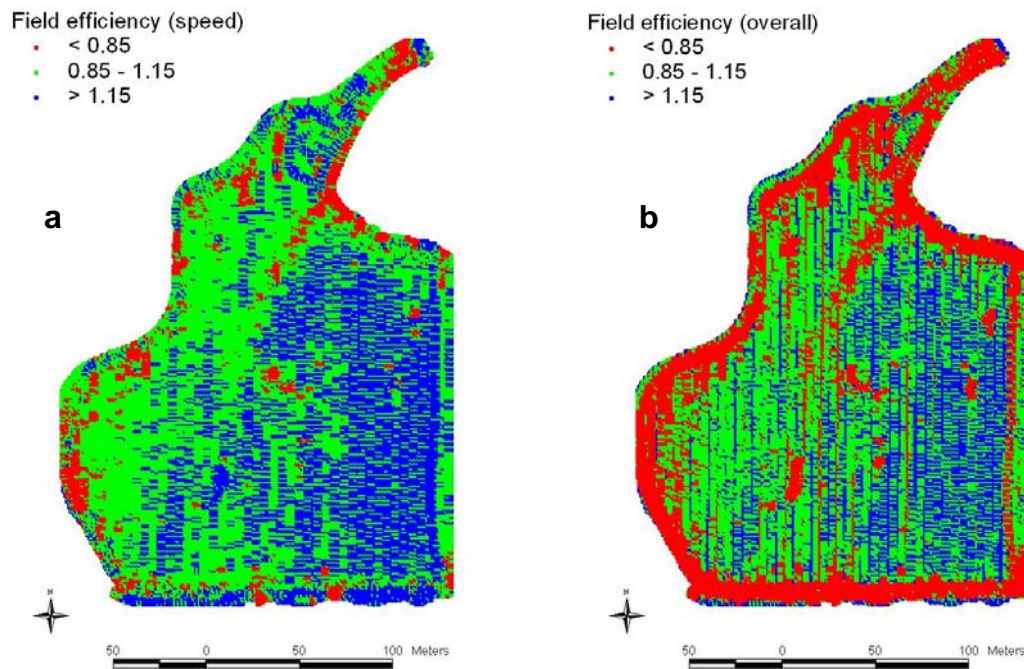


Figure 7. Field efficiency maps representing speed effect (a) and overall performance (b).

Conclusion

The maps presented in this work are examples of various types of information imbedded in the records of geographic positions logged during various field operations. The algorithm developed allows transforming this information into two coverage maps (Coverage 1 and Coverage 2). The first map indicates field areas affected by repeated passes and variable actual swath width. The second map also reflects the effect of variable travel speed. The obtained maps can be converted into a set of data layers associated with conventional categories evaluating machinery performance (cost of operation, capacity, efficiency, etc.). Various types of analytical methods can be used in the future to utilize these data while developing decision-making strategies to improve site-specific crop management.

Acknowledgements

The authors are thankful to Paul Jasa for facilitating the data collection and to Ashish Maheshwari for the initial data processing.

References

- Adamchuk, V.I. 2001. Untangling the GPS data string. Precision Agriculture extension circular EC 01-157. Lincoln, Nebraska: University of Nebraska Cooperative Extension
- ASAE Standards, 49th Edition. 2002a. S495. Uniform terminology for agricultural machinery management. St. Joseph, Michigan: ASAE.
- _____. 2002b. D497.4. Agricultural machinery management data. St. Joseph, Michigan: ASAE.

- Grisso, R.D., P.J. Jasa, and D. Rolofson. 2002. Field efficiency determination from spatial data. *Applied Engineering in Agriculture* 18(2):171-178.
- Grisso, R.D., P.J. Jasa, M.A. Schroeder, M.F. Kocher, and V.I. Adamchuk. 2004. Field efficiency determination using traffic pattern indices. *Applied Engineering in Agriculture* (in press).
- Jose, H.D. and L.J. Brown. 2002. 2002 Nebraska farm custom rates – part II. Extension circular EC02-826-A, Lincoln, Nebraska: University of Nebraska Cooperative Extension
- Renoll, E.S. 1981. Predicting machine field capacity for specific field and operating conditions. *Transactions of the ASAE* 24(1): 45-47.
- Taylor, R.K., M.D. Schrock, and S.A. Staggenborg. 2002. Extracting machinery management information from GPS data. *Paper No. 02-10008*. St. Joseph, Michigan: ASAE.